Morphologies and Mechanical Properties of a Series of Block-Double-Graft Copolymers and Terpolymers

Yuqing Zhu, Roland Weidisch,† and Samuel P. Gido*

Department of Polymer Science & Engineering, University of Massachusetts, Amherst, Massachusetts 01002

Gabriel Velis and Nikos Hadjichristidis*

Department of Chemistry, University of Athens, Panepistimiopolis Zografou 15771, Athens, Greece

Received March 6, 2002

ABSTRACT: Morphological characteristics and mechanical properties of a series of block-double-graft (BDG) copolymers and terpolymers polystyrene−[1,2-polybutadiene-*g*-X_2] (X = 1,4-polybutadiene, polyisoprene, polystyrene, and polystyrene-*b*-polyisoprene diblocks) were investigated by transmission electron microscopy (TEM), small-angle X-ray scattering (SAXS), and tensile testing. All BDG materials have linear polystyrene−1,2-polybutadiene (PS-*b*-1,2-PBD) diblock copolymer backbones. Two identical branches are grafted at every randomly distributed tetrafunctional junction point on the 1,2-PBD part of the backbone. Standard microstructures, such as body-center-cubic spheres, hexagonally packed cylinders, and lamellae, are obtained at different total PS volume fractions. It is found that when the branches are polydienes, the BDG molecules form the same morphologies as their linear diblock counterparts. In such cases, phase separation occurs between the polystyrene domain and a combined diene microdomain formed by the backbone 1,2-PBD part and the polydiene branches. In BDG materials in which the branches are polystyrene−polyisoprene diblock copolymers, lamellae are obtained at a total PS volume fraction close to 0.50. It is found that the domain spacings of these materials are predominately determined by the molecular weights of the diblock branches instead of the backbones. A lamellae-forming BDG terpolymer with an average of three tetrafunctional junction points per molecule exhibited characteristic thermoplastic elastomer properties with a stress at break of 32 MPa and strain at break of 1000%. It is proposed that the high strength of this BDG terpolymer is attributed to the chain conformation in the microphase-separated state. The elastic PBD blocks of the backbone bridge adjacent PS domains through multiple junction points, resulting in the enhanced elastomeric properties. Several parameters are found to influence the mechanical properties of these BDG materials: (1) the existence of backbone PS, (2) the molecular weight of the branches, and (3) the number and functionality of branch points on the 1,2-PBD part of the backbone.

I. Introduction

Molecular architecture plays an important role in determining morphology, phase behavior, and material properties of block copolymers. While the morphology of linear, conformationally symmetric diblock copolymers relies entirely on the volume fraction of the respective blocks,[1−4] the morphology of single-graft and A_mB_n star-block copolymers also depends on an additional factor—the molecular asymmetry parameter, $\epsilon = (n_A/n_B)(l_A/l_B)^{1/2}$. The ratio of number of arms of the two block types (n_A/n_B) represents the asymmetry due to the architecture. The conformational asymmetry between the two block materials is expressed by the ratio $(l_A/l_B)^{1/2}$, where l_i is the ratio of segmental volume to the square of statistical segment length for the block material i.[4] At $\epsilon = 1$, conformationally symmetric, AB diblock behavior is observed with the morphology windows being symmetric around 0.5 volume fraction. However, as one increases the arm number of one species relative to the other, the morphological behavior may become strongly asymmetric with respect to volume fraction. Hence, branched block copolymers are able to yield morphologies that cannot be formed by linear diblock copolymers at the same volume fractions.

In linear ABC triblock copolymer systems, the molecular architecture, the three interaction parameters between different pairs of polymer blocks, and the volume fraction of each block combine to yield fascinating nanoscale morphologies.[5−10] While most studies on block copolymers are focused on the influence of chain architecture on phase behavior and morphology, far fewer have focused on the correlations among molecular architecture, the microstructure thus obtained, and the resulting mechanical properties.[11−16] This lack of well-controlled studies linking molecular architecture to mechanical properties no doubt is the result of the difficulties inherent in synthesizing even small amounts of molecules of highly controlled yet complex molecular architecture. While such small quantities of material are sufficient for morphological study, they are generally not sufficient for mechanical properties evaluation.

The influences of molecular architecture on mechanical properties of block copolymers can be demonstrated by the higher tensile strength obtained by triblock copolymers with a glassy−rubbery−glassy block sequence compared to diblocks of similar composition and molecular weight.[17] The rubbery middle block of a triblock copolymer produces bridges between glassy domains, thereby creating a physically cross-linked

† Present address: Institut für Polymerforschung Dresden (IPF), Teilinstitut Physikalische Chemie und Physik der Polymere, Hohe Strasse 6, 01069 Dresden, Germany.

* To whom correspondence should be addressed: e-mail spgido@squeaky.pse.umass.edu.

10.1021/ma020345x CCC: $22.00
Published on Web 06/19/2002

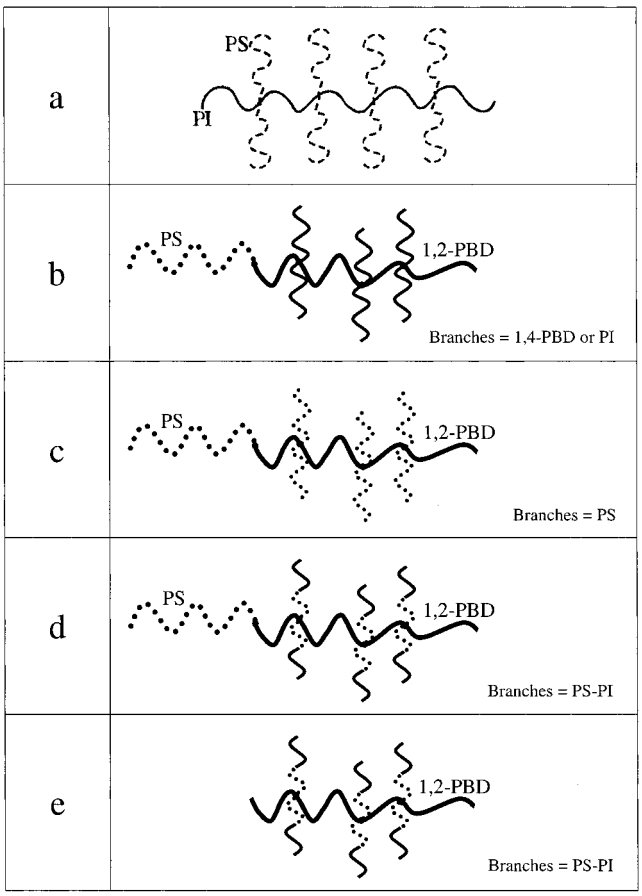

Figure 1. Illustrations of (a) a multigraft copolymer PS-*g*-PI_2 with regularly spaced, tetrafunctional junction points; (b) a BDG copolymer with branch X = 1,4-PBD or PI; (c) a BDG copolymer with branch X = PS; (d) a BDG terpolymer with branch X = PS−PI; and (e) a HDG terpolymer having a 1,2-PBD backbone and PS−PI branches.

nanocomposite system which can be processed at elevated temperatures. The rubbery block of diblock copolymers, on the other hand, possesses a covalent bond to only one of the adjacent glassy domains and thus is not able to form this physically cross-linked network. Similar conclusions have been reached comparing weakly segregated poly(styrene-*b*-butyl methacrylate) (PS−PBMA) diblocks and PBMA−PS−PBMA triblock copolymer systems. Recently, mechanical properties of a group of tetrafunctional multigraft PI-*g*-PS_2 copolymers, with the molecular architecture illustrated in Figure 1a, have been studied by Weidisch et al.[18] These results indicate that higher numbers of junction points per molecule, as well as the fact that there are two PS branches per junction point, enhance energy transfer from the rubbery matrix to the glassy domains. Molecular architecture is not the only factor that can affect material properties. Since the glassy domains act as the reinforcing component, their shape, orientation, and connectivity with respect to the loading direction significantly influence mechanical properties. Block copolymers with the three-dimensional gyroid morphology were found to have enhanced tensile properties compared to block copolymers with other morphologies.[19] In this case, this phenomenon was attributed to the specific gyroid microdomain geometry rather than the PS content, molecular architecture, or molecular weight. Additionally, a PS−PBMA diblock copolymer material with PBMA cylinders was found to exhibit higher tensile strength than pure polystyrene.[13] This phenomenon was credited to the phase behavior and interface formation in the diblock copolymer. All these results indicate that by tailoring molecular architecture, which in turn controls morphology and microstructure, mechanical properties of block copolymers can be controlled and enhanced.

Recently, a series of A-(B-*g*-X_2) block-double-graft (BDG) copolymers and terpolymers have been synthesized by using chlorosilane coupling strategies.[20] The molecular architectures of these materials are illustrated in Figure 1b−d. These molecules have low-polydispersity polystyrene-*b*-1,2-polybutadiene (PS-1,2-PBD) backbones. On the 1,2-PBD part of the backbone, there are several tetrafunctional junction points with two branches grafted on each. Different branch materials were used in the various samples of this study including 1,4-PBD (b), PI (b), PS (c), and PS−PI linear diblock copolymers with the PS block grafted directly to the backbone (d). The placement of the junction points along the 1,2-PBD part of the backbone is determined by the hydrosilylation reaction of vinyl groups of the 1,2-PBD part of the backbone. Coupling of two living branches to each of these hydrosilylated groups leads to the formation of randomly located tetrafunctional junction points. The architecture combines features of linear diblock and graft block copolymers, offering novel opportunities to study the influence of polymer molecular architecture on morphology and in turn on material properties. The present study focuses on the influence of architecture on morphology and on the tensile properties of copolymers and terpolymers of BDG architecture. For comparison, a homo-double-graft (HDG) terpolymer 1,2-PBD-*g*-$(PS-PI)_2$ is also studied. The molecular architecture of this material is shown in Figure 1e. It consists of the same 1,2-PBD backbone with grafted PS−PI diblocks as in Figure 1d, but it lacks the PS backbone block.

II. Experimental Section

Synthesis and Molecular Characterization. Details of the synthesis of these block-double-graft copolymers and terpolymers were described in an early paper.[20] Polymerization and linking reactions were carried out in evacuated, *n*-BuLi-washed, and solvent-rinsed glass reactors. The purification of the monomers, solvents, and linking and terminating agents to the standards required for high-vacuum techniques has been described elsewhere.[21] More details about the controlled hydrosilylation reaction were given previously.[21] To obtain the 1,2-microstructure and thus facilitate the hydrosilylation of the 1,2-PBD blocks, polymerization of butadiene was carried out in the presence of dipiperidinoethane.[20,22,23]

Molecular characteristics of BDG copolymers and terpolymers, the HDG terpolymer, and precursor intermediate building blocks of these structures are listed in Table 1. Membrane osmometry (MO) was performed in toluene at 35 °C, and vapor pressure osmometry (VPO) was performed at 35 °C in toluene. Size-exclusion chromatography (SEC) analysis with both refractive index and UV detectors ($\lambda = 262$ nm) were performed in tetrahydrofuran (THF) at 30 °C. Microstructures of polydiene blocks were obtained from ^{1}H NMR in $CDCl_3$ at 30 °C (with a Varian Mercury instrument at 200 MHz). These results are as follows: 100 wt % 1,2-addition for 1,2-PBD backbone blocks, 92 wt % 1,4-addition and 8 wt % 1,2-addition for all 1,4-PBD branches, and 93 wt % 1,4-addition and 7 wt % 3,4-addition for PI branches.

All the BDG materials in this study were synthesized from three PS-1,2-PBD backbones which are listed in Table 1 as backbone-1−3. In Table 1, each backbone is followed by the BDG material(s) that was/were synthesized from it. A PS-[1,2-

Table 1. Molecular Characteristics of the Precursors and the Fractionated BDG Copolymers and Terpolymers

		branches		BDG copolymer or terpolymer			
	sample	M_n[c] ($\times 10^{-3}$)	M_w/M_n[e]	M_n[c] ($\times 10^{-3}$)	M_w/M_n[e]	wt % PS ^{1}H NMR	f
	PS-1,2-PBD backbone-1	20.5,[a] 56.0[b]	1.03			36	
BDG1	PS-[1,2-PBD-*g*-(1,4-PBD)$_2$]-1	3.0	1.06	84.2	1.05	35	5
	PS-1,2-PBD backbone-2	7.30,[a] 24.6[b]	1.02			30	
BDG2	PS-[1,2-PBD-*g*-(1,4-PBD)$_2$]-2	3.0	1.06	53.1	1.05	19	5
	PS-1,2-PBD backbone-3	24.5,[a] 39.9[b]	1.04			62	
BDG3	PS-[1,2-PBD-*g*-(1,4-PBD)$_2$]-3	2.30[d]	1.07	84.2	1.05	32	10
BDG4	PS-[1,2-PBD-*g*-(PI)$_2$]	13.2	1.04	288	1.05	11	9
BDG5	PS-[1,2-PBD-*g*-(PS)$_2$]	5.0[d]	1.08	157	1.06	89	12
BDG6	PS-[1,2-PBD-*g*-(PS−PI)$_2$]-1	14.0	1.06	280	1.08	52	9
BDG7	PS-[1,2-PBD-*g*-(PS−PI)$_2$]-2	32.8	1.04	226	1.06	48	3
	1,2-PBD backbone	17.5	1.03				
HDG	1,2-PBD-*g*-(PS−PI)$_2$	12.5	1.03	235	1.07	45	9

[a] Molecular weight of PS part of the backbone. [b] Total molecular weight of PS-1,2-PBD backbone. [c] MO in toluene at 30 °C. [d] VPO in toluene at 50 °C. [e] SEC in THF at 30 °C. [f] Number of double grafts per molecule: $[(M_n)_{BDG} - (M_n)_{backbone}]/[2(M_n)_{branch}]$.

Table 2. Morphological Characteristics of BDG and HDG Molecules

	sample	morphology	d^* (Å)[a]	vol % PS	vol % PBD	vol % PI
BDG1	PS-[1,2-PBD-*g*-(1,4-PBD)$_2$]-1	PS cylinders	381	22.5	77.5	
BDG2	PS-[1,2-PBD-*g*-(1,4-PBD)$_2$]-2	PS spheres	230	12.6	87.4	
BDG3	PS-[1,2-PBD-*g*-(1,4-PBD)$_2$]-3	PS cylinders	335	27.0	73.0	
BDG4	PS-[1,2-PBD-*g*-(PI)$_2$]	random PS spheres	268	7.60	5.30	87.1
BDG5	PS-[1,2-PBD-*g*-(PS)$_2$]	disordered		89.2	10.8	
BDG6	PS-[1,2-PBD-*g*-(PS−PI)$_2$]-1	lamellae	175	48.8	5.70	45.5
BDG7	PS-[1,2-PBD-*g*-(PS−PI)$_2$]-2	lamellae	244	44.9	7.10	48.0
HDG	1,2-PBD-*g*-(PS−PI)$_2$	lamellae	167	41.9	7.7	50.4

[a] Primary SAXS reflection, $d^* = 2\pi/q^*$.

PBD-*g*-(1,4-PBD)$_2$] material was produced on the basis of each of the three backbones. These molecules have different branch molecular weight, number of branches, and total PS volume fractions; they are labeled PS-[1,2-PBD-*g*-(1,4-PBD)$_2$]-1 to 3 according to their respective backbones. Two different BDG terpolymer molecules that were synthesized on the basis of PS-1,2-PBD backbone-3 have the same molecular structure but different branches and total PS volume fractions. They are labeled PS-[1,2-PBD-*g*-(PS−PI)$_2$]-1 and -2, respectively.

Morphological Characterization and Tensile Testing. To prepare specimens for both morphological characterization and tensile testing, all the copolymer samples were dissolved in toluene to produce 5 wt % solutions. Solvent evaporation was controlled so that it occurred over 2 weeks at room temperature, yielding films about 0.7 mm thick. The dried films were then annealed at 120 °C under high vacuum for 5 days to further promote equilibrium microstructures. GPC was performed on all samples after casting and thermal annealing. No change in molecular weight was observed as a result of these treatments. Thin sections 50−100 nm thick were prepared by cryo-ultramicrotoming the bulk films using a Leica EM-FCS microtome, equipped with a crygenic sample chamber operated at −110 °C. These sections were collected and stained by osmium tetraoxide vapor for 6 h. TEM studies were performed using a JEOL 100 CX transmission electron microscope operated at 100 kV.

Small-angle X-ray scattering (SAXS) measurements were carried out at the National Synchrotron Light Source (NSLS) at Brookhaven National Laboratory (BNL) beamline X27C, Upton, NY, and at University of Massachusetts−Amherst (UMass). The wavelength of the X-ray beam used in BNL was 1.307 Å, and the sample-to-detector distance was determined to be 1513 mm. Two-dimensional scattering patterns were recorded on Fujitsu HR-V image plates and were digitized using a Fujitsu BAS 2000 image plate reader. Background was subtracted, circular averaging was performed, and the data were plotted as log I vs q. Ni-filtered Cu Kα radiation (1.54 Å wavelength) from a Rigaku rotating anode (operated at 40 kV, 200 mA) was used for SAXS studies at UMass. The primary beam was collimated by a set of three pinholes. A gas-filled area detector (Siemens Hi-Star), located at 875.2 mm from the sample, was used to record scattering patterns. The peak positions were determined by fitting scattering curves with an exponential background function and Gaussian peaks using the Peakfit program. The uncertainty of q value is ±0.0003 Å^{-1}.

Morphological results for each sample and its corresponding volume fractions are given in Table 2. For easy identification in the paper, we label these BDG copolymers and terpolymers BDG1 to BDG7. Names and corresponding molecular formulas for each sample can be found in Tables 1 and 2. Tensile testing on BDG terpolymers BDG6 and BDG7 as well as the HDG was performed using a universal testing machine Instron 1123 with a 1000 N load cell at a crosshead speed of 15 mm/min. Dog bone specimens of 0.7 mm thick were stamped from the same pieces of cast and annealed film that were used for TEM and SAXS studies with a standard die having 20 mm gauge length. Crosshead separation was used to quantify strain. This approach may slightly overestimate strain due to such effects as slippage in the grips, often found with elastomers. Dog bone samples were glued into the grips to minimize this problem. Material stress vs strain curves were produced by utilizing engineering stresses based on the measured initial cross-section dimensions of these specimens. For each material, at least 10 tests were performed.

III. Results and Discussion

Morphology. Morphological results of BDG and HDG copolymers and terpolymers reveal the formation of standard microstructures (Table 2). To discuss their morphologies and tensile behaviors, these materials are separated into three groups according to the type of their branches.

The first group of BDG molecules consists of BDG1 though BDG4, whose branches are either 1,4-PBD (BDG1 through BDG3) or PI (BDG4) homopolymers. On the basis of TEM images, it is found that BDG1 and BDG3 form hexagonally packed PS cylinders, and BDG2 forms body-center-cubic (bcc) PS spheres. TEM results of BDG4 are consistent with microphase-separated PS spheres in a polydiene matrix, without long-range lattice order. Figure 2 presents representative TEM images of BDG2 (a), BDG3 (b), and BDG4 (c). TEM images of

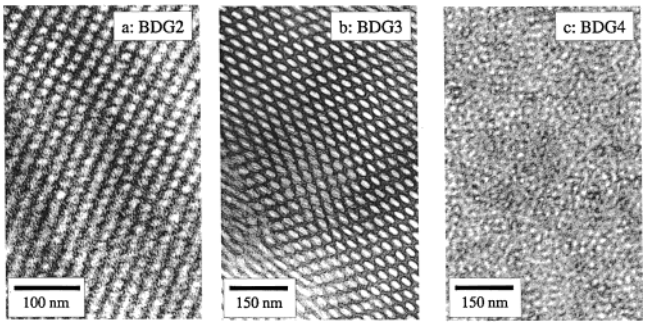

Figure 2. TEM images of (a) BDG2, (b) BDG3, and (c) BDG4.

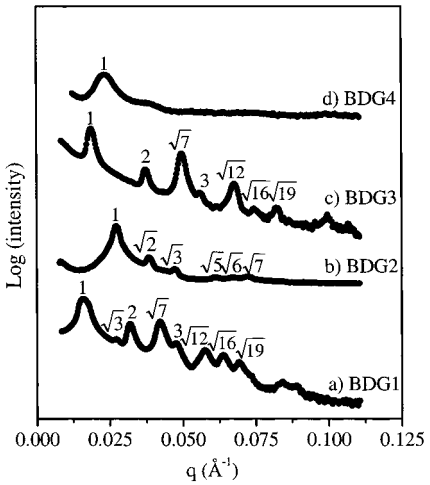

Figure 3. Small-angle X-ray scattering data of (a) BDG1, (b) BDG2, (c) BDG3, and (d) BDG4.

BDG1 are similar to those of BDG3. In Figure 3, multiple higher order reflections can be readily observed in SAXS profiles of BDG1, BDG2, and BDG3. BDG1 exhibits Bragg reflections with ratios q_n/q^*, of the nth reflection scattering vector to the scattering vector of the primary peak, of 1, $\sqrt{3}$, $\sqrt{4}$, $\sqrt{7}$, $\sqrt{9}$, $\sqrt{12}$, $\sqrt{16}$, and $\sqrt{19}$, indicative of a hexagonal morphology. The (100) interplanar spacing in BDG1 is calculated to be 381 Å. BDG3 exhibits a similar sequence of scattering vector ratios suggestive of hexagonal morphology, except that the $\sqrt{3}$ peak is missing. The comparison to TEM images confirms the hexagonally packed cylindrical structure, and we thus conclude that the missing $\sqrt{3}$ peak is due to a minimum in the form factor at the volume fraction of the sample.[24] BDG3 has a (100) spacing of 335 Å. BDG2 gives relative positions of primary and higher-order reflections at 1, $\sqrt{2}$, $\sqrt{3}$, $\sqrt{5}$, $\sqrt{6}$, and $\sqrt{7}$, consistent with bcc spherical structure. Based on the data, the primary scattering peak gives a (110) interplanar spacing of 230 Å, which corresponds to a cubic lattice parameter of 325 Å. Scattering data of BDG4, shown in Figure 3, display a broad primary peak and an additional broad, higher angle peak due to the form factor. This scattering profile is consistent with its TEM image in Figure 2, which shows a microphase-separated morphology that lacks long-range lattice order. The primary scattering peak suggests an average correlation length of 268 Å for BDG4, and the broad higher q reflection is consistent with form factor scattering from spherical domains. The TEM image of BDG4 in Figure 2 is similar to previously reported images of microphase-separated spherical domains without lattice order.[25]

The morphological behaviors of BDG1−BDG3 are similar to those of their respective linear diblock copolymer counterparts with the same PS volume fractions. The PS volume fractions of the cylinder-forming BDG samples BDG1 and BDG3 are 0.23 and 0.27, respectively, falling in the same range where linear diblocks would also form cylinders.[1,2,24] BDG2, which forms a spherical microstructure, has a PS volume fraction 0.13, falling in the same range where linear diblocks would also form spheres. The fact that these BDG molecules behave as their linear counterparts with similar PS volume fraction suggests that microphase separation is occurring between PS and a mixed matrix of 1,2-PBD and 1,4-PBD.

A simple χN calculation confirms the miscibility between 1,2-PBD and 1,4-PBD inside the matrices phases of BDG1−BDG3. The 1,2-PBD/1,4-PBD part of molecule has the architecture of a multigraft copolymer 1,2-PBD-*g*-(1,4-PBD)$_2$ with 1,2-PBD as its backbone and two 1,4-PBD homopolymer branches grafted at every randomly spaced junction point. It has been shown experimentally[25−27] and theoretically[28] that the appropriate basis for calculating the χN of a graft copolymer is the *constituting unit* composed of the average structure per junction point. Accordingly, the constituting block copolymer units in BDG1, BDG2, and BDG3 are four-arm, *miktoarm* stars of the type (1,2-PBD)$_2$-(1,4-PBD)$_2$. Roughly speaking, a symmetric four-arm *miktoarm* star will display morphological and phase segregation characteristics similar to the corresponding (1,2-PBD)−(1,4-PBD) diblock where the block lengths are equal to those of the various star arms.[25,28−32] Thus, the calculation of χN for a (1,2-PBD)$_2$−(1,4-PBD)$_2$ is approximated by the χN of this corresponding diblock. The interaction parameter χ between 1,2-PBD and 1,4-PBD can be calculated on the basis of the equation derived by Sakurai and co-workers.[33]

$$\chi_{1,2-1,4} = 2.69 \times 10^{-3} + 1.87/T$$

Based on this expression for χ and the degrees of polymerization of the various diblocks, χN values at 25 °C are as follows: 1.1 (BDG1), 0.82 (BDG2), and 0.53 (BDG3). These χN values clearly indicate that the 1,2-PBD backbone and 1,4-PBD branches in these three molecules are highly miscible. On the other hand, a calculation of the χN at 25 °C between PS and a mixed PBD domain type indicates relatively strong segregation.[34] These values are as follows: 90 (BDG1), 61 (BDG2), and 88 (BDG3).

A similar approach can also be applied to the evaluation of block miscibility and/or degree of segregation for BDG4. In the graft part of this molecule the branches are PI homopolymers, and the constituting block copolymer unit is (1,2-PBD)$_2$−PI$_2$. On the basis of the interaction parameter between isoprene and butadiene reported by Floudas,[35] χN of the constituting block copolymer in the graft part of BDG4 is found to be 0.27. Furthermore, it is well-known that the miscibility of PBD with PI increases with increasing vinyl content (1,2-addition) in PBD.[36] The blend of PI and PBD even exhibits a negative χ parameter when the vinyl content of PBD is over 90%.[37,38] Our well-controlled synthetic technique allows strict 1,2-addition of butadiene monomers onto the backbone, and thus the vinyl contents of backbone 1,2-PBD in all BDG molecules approach 100%. This process will produce a very low enthalpic interaction between isoprene and butadiene. On the basis of these arguments, we believe that the two rubbery

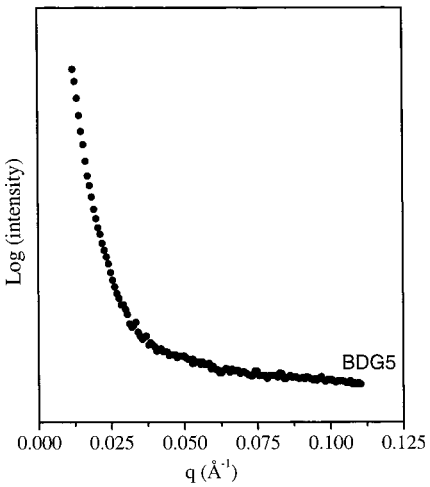

Figure 4. Small-angle X-ray scattering profile for BDG5.

components in BDG4 are also miscible with each other. Once again, if we can lump together PI and backbone 1,2-PBD and calculate the χN between PS and the combined rubbery phase, we find that the system has an χN of 188 at the annealing temperature of 120 °C. The total volume fraction of PS in BDG4 is only about 0.076 so a diblock analogue would form PS spheres in a polydiene matrix. Our data suggest that spherical domains are indeed formed but that they are unable or organize themselves onto a lattice. Previous work[29,31] has shown examples of other multigraft copolymers in which the expected (based on component volume fractions) microphase-separated domain shape forms, but long-range lattice order is suppressed.

BDG1 through BDG4 all share the same general molecular architecture shown in Figure 1b. The molecular weight of the PI branches in BDG4 (13 200 g/mol) is significantly higher than that of the PBD branches in BDG1 through BDG3 (3000 g/mol maximum). This molecular weight information is listed in Table 1. The molecular weight of the PI branches in BDG4 is higher than the critical molecular weight for PI entanglement,[39] while the molecular weights of the grafted branches in BDG1 though BDG3 are considerably lower than the corresponding PBD entanglement molecular weight. It is suspected that the longer graft chains hindered the kinetics of microphase separation in BDG4. Extending the annealing time to 10 days and increasing the annealing temperature to 140 °C failed to produce an improvement in the long-range order of the BDG4 morphology.

The second sample grouping consists of BDG5 only. It contains a PS-1,2-PBD backbone with two PS branches grafted at every junction point along the PBD part of the backbone. TEM results on BDG5 indicate a totally disordered state, consistent with the small-angle X-ray scattering data shown in Figure 4. The backbone to which the grafts are attached comprises the only 1,2-PBD in the molecule. This 1,2-PBD is only 11 vol % of the material. There are on average 12 junction points along this PBD block, and thus the average molecular weight of the PBD connector between junction points is only 1300 g/mol. The χN value per junction point in the graft part of this molecule (constituting block copolymer unit) is 2.8 at the annealing temperature of 120 °C and 3.8 at room temperature. For such an asymmetric PBD volume fraction, this places the material deep in the disordered region of the morphology

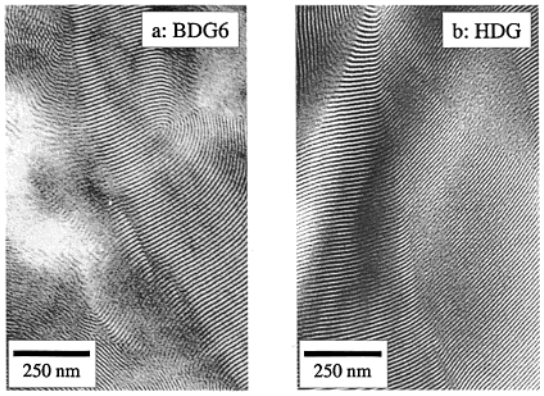

Figure 5. TEM micrographs of (a) BDG6 and HDG.

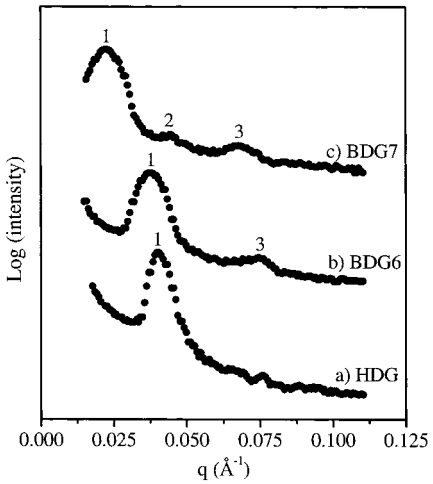

Figure 6. Small-angle X-ray scattering profiles of (a) HDG, (b) BDG6, and (c) BDG7.

diagram. Thus, the lack of microphase-separated structure is not surprising.

The third group of samples consists of BDG6, BDG7, and HDG terpolymers. The branches are PS−PI linear diblock copolymers with the PS blocks of these branches grafting directly onto the PBD parts of the backbones. Lamellae are observed in TEM images of all three materials. Figure 5 shows the TEM images of BDG6 (a) and HDG (b). Small-angle scattering data from BDG6 and BDG7 in Figure 6 display Bragg reflections at integer multiples of the primary reflection q^*, which is consistent with lamellar morphologies. Higher-order reflections in the scattering data from HDG are hard to identify, but TEM micrographs of HDG show well-ordered lamellar structures. Lamellar long periods of BDG6 and BDG7 are 175 and 244 Å, respectively, while that of HDG is 167 Å.

It is found in all TEM micrographs of the materials in the third group that the volume fractions of the PS domains (as compared to the combined, osmium stained, polydiene segments) are close to 0.50. This is consistent with the total PS volume fractions, from backbone and from branches. The observed domain volume fractions suggest that the backbone 1,2-PBD and the PI blocks of the branches remain in the same combined rubbery domain while the PS blocks from both the backbone and branches reside in the other domain. Figure 7a shows some possible chain conformations for BDG6 and BDG7 that arrange the various PS and polydiene blocks among the microphase-separated lamellae of the morphology. Clearly, many possible conformations can occur and are

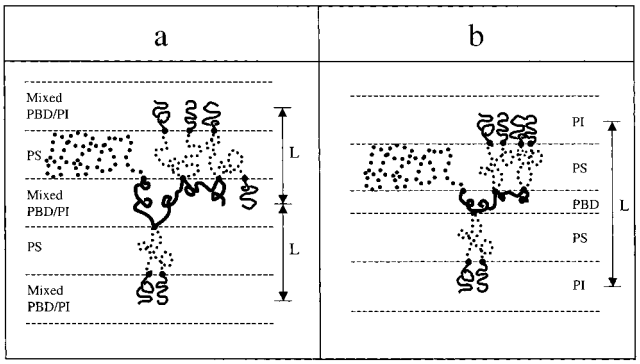

Figure 7. (a) Chain conformation of BDG6 and BDG7 in the microphase-separated state. (b) Illustration of an alternative morphology in which the backbone 1,2-PBD and branch PI blocks form different domains separated by PS domains.

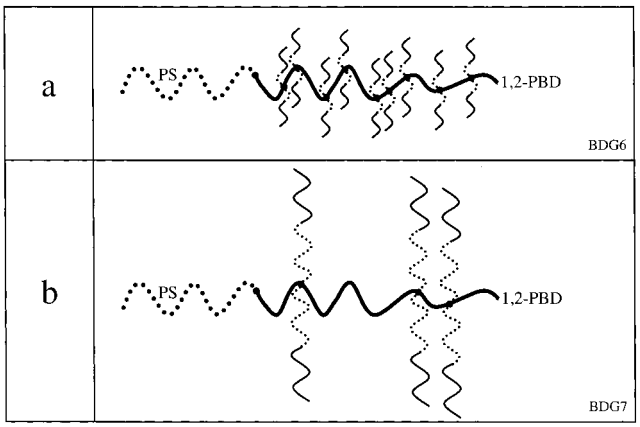

Figure 8. Molecular architectures of (a) BDG6 and (b) BDG7.

statically represented in the material. In some conformations a single molecule can span up to two full long periods of the lamellar structure. This is in contrast to diblocks which only span half a long period and to triblocks which can at most span a full long period. Figure 7b illustrates an alternative morphology in which the backbone 1,2-PBD and branch PI blocks form different domains separated by PS domains. However, for BDG and HDG molecules, the volume percents of the backbone 1,2-PBD blocks are less than 8%. Most of the polydiene content is in the branches. Thus, the formation of separate PBD and PI domains would yield a −PI−PS−PBD−PS−PI− alternating structure, with dramatic domain thickness differences between PBD and PI layers.[40,41] The TEM and scattering results indicate a single type of combined polydiene lamellar layer.

Figure 8 illustrates the differences between BDG6 (a) and BDG7 (b). Both molecules are based on the same PS-1,2-PBD backbone, but the molecular weight of the branches is 14 000 g/mol in BDG6 and is 32 800 g/mol in BDG7. The number of junction points on the backbone 1,2-PBD block is 9 in BDG6 and 3 in BDG7. The lamellar spacing of BDG7 (244 Å) is significantly larger than that of BDG6 (175 Å). We find that the lamellar spacings of BDG6 and BDG7 are comparable to those reported for diblocks of similar molecular weight to those of the diblock branches in BDG6 and BDG7.[42] It seems that the domain spacings of BDG6 and BDG7 are predominately determined by molecular weights of the branches instead of the backbones since BDG6 and BDG7 are built on the same backbone. HDG is very similar to BDG6 in molecular characteristics except that

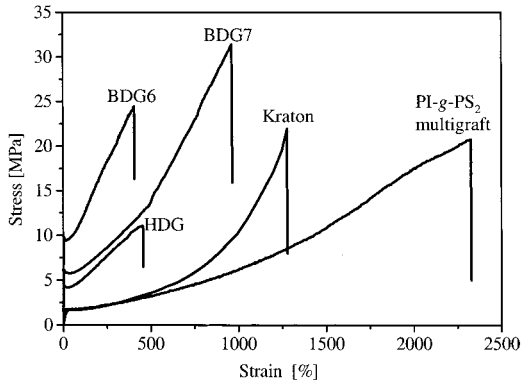

Figure 9. Stress−strain curves for (1) BDG6, 9 junction points, and the branch molecular weight is 14 000 g/mol; (2) BDG7, 3 junction points, and the branch molecular weight is 32 800 g/mol; (3) HDG, 9 junction points, and the branch molecular weight is 12 500 g/mol; (4) Kraton D1101; and (5) PI-*g*-PS_2 multigraft copolymer with 9 junction points at branch molecular weight of 13 000 g/mol.

HDG does not have a backbone PS block. The fact that the HDG lamellar spacing (167 Å) is very similar to that of BDG6 supports the assertion that the characteristics of the grafted diblocks determine this spacing.

Tensile Properties. Figure 9 compares the stress−strain behavior of BDG6, BDG7, and HDG terpolymers, a PI-*g*-PS_2 multigraft copolymer, and a commercial thermoplastic elastomer (TPE)—Shell Kraton D1101. The PI-*g*-PS_2 multigraft copolymer has a total molecular weight of 994 000 g/mol with an average of nine tetrafunctional branch points per molecule and a PS volume fraction of 0.22. It was found to have wormlike cylindrical domains (not ordered on a lattice) of PS in a PI matrix. The morphology and tensile properties of this material have been reported previously.[18] The Kraton used for comparison is a polystyrene−polyisoprene−polystyrene linear triblock copolymer and forms hexagonal PS cylinders in a PI matrix. Styrene mass content is reported by the manufacturer to be 31%. The number-average molecular weight of this Kraton determined via GPC in our laboratory is 1.05×10^5 g/mol. The PI-*g*-PS_2 multigraft copolymer and Kraton were prepared and tested under the same conditions used for BDG6, BDG7, and HDG. Figure 9 shows that HDG displays low strength and a low stain at break. On the other hand, BDG6, BDG7, and Kraton exhibit a large increase of stress at higher strains, typical tensile behavior of thermoplastic elastomers (TPE). BDG7 exhibits higher strength and higher strain at break than BDG6. Its strain at break is a little lower than that of Kraton, but its strength is considerably higher. As previously reported,[18] the PI-*g*-PS_2 multigraft copolymer displays very high strain at break and moderately high strength.

Both BDG6 and BDG7 show excellent TPE properties resulting from the ability of individual molecules to participate in multiple physical cross-links (provided by the PS domains) as illustrated in Figure 7a. Such chain conformations resemble those of PS−PI−PS triblock copolymer TPEs in which the rubbery middle block bridges two glassy domains. In the BDG materials, however, a single molecule provides multiple connections between different glassy PS domains, thus resulting in an improvement in strength.

Compared to BDG7, BDG6 displays lower strength and strain at break. While BDG7 has a lower number

of junction points than BDG6, its PS−PI branches have higher molecular weight than those in BDG6. While it was previously found[18] that a higher number of branch points per molecule improves strength and elongation at break, it is also clear from the results on BDG6 and BDG7 that the molecular weight of grafts must be sufficiently high to entangle and not pull out of the cross-linking domains in order to improve properties. The molecular weights of the PS blocks on the BDG6 branches are lower than the critical molecular weight M_c to achieve chain entanglement (M_c = 17 000 g/mol for PS). For BDG7, on the other hand, the PS blocks on the grafts are 16 000 g/mol, approaching the entanglement molecular weight. This is apparently enough to provide enhancement of properties.

For BDG terpolymers, we found two parameters that can adjust material properties—molecular weight of the branches and molecular architecture. Branches must exceed the entanglement molecular weight in order to provide effective physical cross-links. In terms of molecular architecture, the PS blocks in the branches provide multiple coupling points between PS and rubbery domains, which appear to enhance properties. The number of junction points and the functionality of these junction points are also very important aspects for energy transfer among different domains.

Acknowledgment. The authors thank Sheng Hong for the preliminary morphological characterization of some materials. S.P.G. acknowledges funding from the U.S. Army Research Office and Army Research Laboratory under Contracts DAAD-19-01-1-0544 and DAAD-19-01-2-0002. R.W. acknowledges financial support for Heisenberg fellowship from "Deutsche Forschungsgemeinschaft" (DFG). We also acknowledge the use of central facility and the W. M. Keck Electron Microscopy in the Material Research Science and Engineering Center (MRSEC) at the University of Massachusetts—Amherst.

References and Notes

(1) Helfand, E. *Macromolecules* **1975**, *8*, 552.
(2) Helfand, E.; Wasserman, Z. R. *Macromolecules* **1976**, *9*, 879.
(3) Helfand, E.; Wasserman, Z. R. *Macromolecules* **1980**, *13*, 994.
(4) Milner, S. *Macromolecules* **1994**, *27*, 2333.
(5) Mogi, Y.; Kotsuji, H.; Kaneko, Y.; Mori, K.; Matsushita, Y.; Noda, I. *Macromolecules* **1992**, *25*, 5408.
(6) Gido, S. P.; Schwark, D. W.; Thomas, E. L. *Macromolecules* **1993**, *26*, 2636.
(7) Stadler, R.; Auschra, C.; Beckmann, J.; Krappe, U.; Voigt-Martin, I.; Leibler, L. *Macromolecules* **1995**, *28*, 3080.
(8) Krappe, U.; Stadler, R.; Voigt-Martin, I. *Macromolecules* **1995**, *28*, 4558.
(9) Zheng, W.; Wang, Z. *Macromolecules* **1995**, *28*, 7215.
(10) Breiner, U.; Krappe, U.; Stadler, R. *Macromol. Rapid Commun.* **1996**, *17*, 567.
(11) Alward, D. B.; Kinning, D. J.; Thomas, E. L.; Fetters, L. J. *Macromolecules* **1986**, *19*, 215.
(12) Kinning, D. J.; Thomas, E. L.; Alward, D. B.; Fetters, L. J.; Handlin, D. L. *Macromolecules* **1986**, *19*, 1288.
(13) Weidisch, R.; Michler, G. H.; Arnold, M.; Fisher, H. *J. Mater. Sci.* **2000**, *35*, 1257.
(14) Weidisch, R.; Schreyeck, G.; Ensslen, M.; Michler, G. H.; Stamm, M.; Schubert, D. W.; Budde, H.; Horing, S.; Arnold, M.; Jerome, R. *Macromolecules* **2000**, *33*, 5495.
(15) Weidisch, R.; Michler, G. H.; Arnold, M. *Polymer* **2000**, *41*, 2231.
(16) Sakurai, S.; Sakamoto, J.; Shibayama, M.; Nomura, S. *Macromolecules* **1993**, *26*, 3351.
(17) Holden, G.; Legge, N. R. In *Thermoplastic Elastomers*; Holden, G., Legge, N. R., Quirk, R., Schroeder, H. E., Eds.; Hanser: Munich, 1996; p 47.
(18) Weidisch, R.; Gido, S. P.; Uhrig, D.; Iatrou, H.; Mays, J.; Hadjichristidis, N. *Macromolecules* **2001**, *34*, 6333.
(19) Dair, B. J.; Honeker, C. C.; Alward, D. B.; Avgeropoulos, A.; Hadjichristidis, N.; Fetters, L. J.; Capel, M.; Thomas, E. L. *Macromolecules* **1999**, *32*, 8145.
(20) Velis, G.; Hadjichristidis, N. *J. Polym. Sci., Part A: Polym. Chem.* **2000**, *38*, 1136.
(21) Morton, M.; Fetters, L. J. *J. Rubber Chem. Technol.* **1975**, *48*, 359.
(22) Halasa, A. F.; Lohr, D. F.; Hall, J. E. *J. Polym. Sci., Polym. Chem. Ed.* **1981**, *19*, 1357.
(23) Bywater, S.; Mackerron, D. H.; Worsfold, D. J. *J. Polym. Sci., Polym. Chem. Ed.* **1985**, *23*, 1997.
(24) Funaki, Y.; Kumano, K.; Nakao, T.; Jinnai, H.; Yoshida, H.; Kimishima, K.; Tsutsumi, K.; Hirokawa, Y.; Hashimoto, T. *Polymer* **1999**, *40*, 7147.
(25) Beyer, F.; Gido, S. P.; Büschl, C.; Iatrou, H.; Uhrig, D.; Mays, J. W.; Chang, M.; Garetz, B. A.; Balsara, N.; Beck Tan, N.; Hadjichristidis, N. *Macromolecules* **2000**, *33*, 2039.
(26) Lee, C.; Gido, S. P.; Poulos, Y.; Hadjichristidis, N.; Beck Tan, N.; Trevino, S. F.; Mays, J. W. *Polymer* **1998**, *39*, 4631.
(27) Gido, S. P.; Lee, C.; Pochan, D. J.; Pispas, S.; Mays, J. W.; Hadjichristidis, N. *Macromolecules* **1996**, *29*, 7022.
(28) Shinozaki, A.; Jasnow, D.; Balazs, A. *Macromolecules* **1994**, *27*, 2496.
(29) Xenidou, M.; Beyer, F. L.; Hadjichristidis, M.; Gido, S. P.; Beck Tan, N. *Macromolecules* **1998**, *31*, 7659.
(30) Olvera de la Cruz, M.; Sanchez, I. C. *Macromolecules* **1986**, *19*, 2501.
(31) Beyer, F. L.; Gido, S. P.; Uhrig, D.; Mays, J. W.; Beck Tan, N.; Trevino, S. F. *J. Polym. Sci., Part B: Polym. Phys.* **1999**, *37*, 3392.
(32) Beyer, F. L.; Gido, S. P.; Poulos, Y.; Avgeropoulos, A.; Hadjichristidis, N. *Macromolecules* **1997**, *30*, 2373.
(33) Sakurai, S.; Hasegawa, H.; Hashimoto, T.; Hargis, I. G.; Aggarwal, S. L.; Han, C. C. *Macromolecules* **1990**, *23*, 451.
(34) Wolff, T.; Burger, C.; Ruland, W. *Macromolecules* **1993**, *26*, 1707.
(35) Floudas, G.; Hadjichristidis, N.; Iatrou, H.; Pakula, T.; Fisher, E. W. *Macromolecules* **1994**, *27*, 7735.
(36) Trask, C. A.; Roland, C. M. *Polym. Commun.* **1988**, *29*, 332.
(37) Roland, C. M. *Macromolecules* **1987**, *20*, 2557.
(38) Tomlin, D. W.; Roland, C. M. *Macromolecules* **1992**, *25*, 2994.
(39) Buzza, D. M. A.; Fzea, A. H.; Allgaier, J. B.; Young, R. N.; Hawkins, R. J.; Hamley, I. W.; McLeish, T. C. B.; Lodge, T. P. *Macromolecules* **2000**, *33*, 8399.
(40) Gido, S. P. *Nature (London)* **1999**, *398*, 107.
(41) Goldacker, T.; Abetz, V.; Stadler, R.; Erukhimovich, I.; Leibler, L. *Nature (London)* **1999**, *398*, 137.
(42) Hashimoto, T.; Shibayama, M.; Kawai, H. *Macromolecules* **1980**, *13*, 1237.

MA020345X